Cite this as: Materials Research Bulletin
Volume 122, 2020, 110683

https://doi.org/10.1016/j.materresbull.2019.110683

Sensitizing, sensing and chemical separation of Tb(III) ions: All in a novel copper metal-organic framework

Faezeh Moghzi[a], Janet Soleimannejad[a,*], Eva Carolina Sañudo[b], Jan Janczak[c]

[a] School of Chemistry, College of Science, University of Tehran, P.O. Box 14155-6455, Tehran, Iran
[b] Departament de Química Inorgànica i Institut de Nanociència i Nanotecnologia, Universitat de Barcelona, Av. Diagonal 645, 08028, Barcelona, Spain
[c] Institute of Low Temperature and Structure Research, Polish Academy of Science, Oko'lna 2, 50-950, Wroclaw, Poland

ARTICLEINFO

Keywords:
Metal-organic framework
Chemical sensing and separation
Fluorescence
Terbium
Copper
Cation exchange

ABSTRACT

The importance of rare earth elements in high-tech materials has promoted the necessity to develop new materials for sensing and separating them. Luminescent metal-organic frameworks (MOFs) due to their promising applications as functional materials for chemical sensing and separation, which upon introducing analytes create multi-responsive systems, have been receiving great attention by scientists. In this regard, we have designed and synthesized a novel three-dimensional copper framework, $[Cu_2(3,4\text{-pydc})_2(H_2O)_5]_n.2nH_2O$ (1; 3,4-H_2pydc = 3,4-pyridine dicarboxylic acid), in ambient condition with an interesting topology and potential application as a cation exchange material. Upon Tb^{3+} ions uptake, compound 1 exhibited the antenna effect to sensitize Tb^{3+} ions and its fluorescent emission was enhanced. It also showed selective sensing ability based on turn-on fluorescence response towards Tb^{3+} ions, in a mixture of main and transition metal ions and Tb^{3+} ions. Furthermore, the results showed that the Tb^{3+} ion exchange process is reversible. Therefore, compound 1 is a promising multifunctional luminescent MOF for simultaneous sensing and chemical separation of Tb^{3+} ions which is an advantage over the previously used MOFs in this regard. Furthermore, the reusability experiment demonstrated that 1 can be utilized for long-term detection and separation of Tb^{3+} ions.

1. Introduction

Because of unique optical, electrical, chemical and magnetic properties of lanthanide ions, they have a key role in many high-tech industries and have been widely used in electronics, laser, and potent magnets [1–3]. Considering the increasing use of lanthanides, the detection and recovery of these rare earth elements is an urgent challenge. In terms of sustainable technologies, the lanthanides are recovered mostly by adsorption, ionic exchange, solvent extraction, and other chemical techniques [4–10]. Amongst these methods, adsorption is one of the most economically efficient techniques with a simple and convenient experimental procedure. Until now, diverse adsorbents such as ion exchange resins and activated carbon and hybrid materials have been utilized for lanthanide separation [11–15]. Because of the low adsorption capacity and poor reusability of the aforementioned materials, the design of new alternative materials with those desirable properties still matters.

Metal-organic frameworks (MOFs) are advanced supramolecular compounds constructed from organic bridging ligands and metal centers that have spun promising application areas such as separation, gas storage, drug delivery, sensing, catalysis, electronics, optics, and photonics as pioneering porous materials [16–22]. Such potential applications have stemmed from their spectacular properties including tunable synthesis, pre-designed secondary building blocks, structural versatility, host-guest interactions and other desirable functionalities [23]. The structural engineering of metal-organic frameworks based on the choice of either organic ligands or metal centers has triggered researchers' interest in achieving a targeted design with unique properties [23]. In the adsorption process of the diverse species, however, the structural architecture has a key role which can be modified by alteration of the functional groups, pore size and the coordination sphere of metal centers [24].

The adsorption of the guest molecule can change the physical or chemical properties of the metal-organic frameworks, which could lead to their utilization as a physical or chemical sensor [25–28]. Luminescent MOFs have the potential to be used as chemosensors due to their functional porous surfaces, available interaction sites and large π-conjugation which enables them to distinguish changes through the host-guest supramolecular interactions [29–31]. MOFs as fluorescent sensors have been widely utilized to detect diverse analytes such as volatile

* Corresponding author.
E-mail address: janet_soleimannejad@khayam.ut.ac.ir (J. Soleimannejad).
Received 10 August 2019; Received in revised form 30 October 2019; Accepted 1 November 2019

organic compounds, cations, and anions because of their high selectivity, sensitivity and rapid response. Among cations, Cd^{2+}, Fe^{3+}, Cu^{2+}, Pb^{2+}, Hg^{2+} and Ag^{+} have mainly been investigated and their sensing using MOFs are mostly based on fluorescence quenching [32–38]. However, the study of MOF-based sensors for simultaneous sensitizing, sensing and also separation of lanthanides has seldom been reported [39,40].

Herein we report the synthesis, crystal structure, and photoluminescence properties of a new 3D metal-organic framework $[Cu_2(3,4\text{-pydc})_2(H_2O)_5]_n.2nH_2O$ (1). Compound 1 has a special topology and hence cationic exchange potential, therefore, its sensing ability towards a diverse range of cations was examined. Remarkable sensitizing ability towards Tb^{3+} ion, sensing and separation details and also reusability of 1 were studied.

2. Experimental

2.1. Material and methods

All reagents and solvents were procured from commercial suppliers and were used without further purification.

Powder X-ray diffraction patterns (PXRD) were recorded on a PANalytical X'Pert PRO MRD (Multipurpose Diffractometer) (Malvern PANalytical, Dusseldorf, Germany) equipped with a CuK_α radiation source ($\lambda = 1.54184$ Å). FT-IR spectra were recorded on a Tensor 27 FT-IR spectrometer (Bruker) in the range of 400-4000 cm^{-1} by utilizing KBr pellets. UV–vis spectra of the solutions were obtained from a Varian Cary 100 spectrophotometer. Fluorescence measurements were carried out on a NanoLogTM-Horiba JobinYvon iHR320 spectrophotometer. Both absorption and fluorescence measurements were recorded at room temperature. Elemental analyses (C, H and N) were executed using a Flash EA® Eager 300–1112 CHNSO analyzer. Inductively coupled plasma mass spectrometry (ICP-MS) was accomplished using a NexION 2000 Perkin-Elmer instrument. TGA-DSC analysis was performed on an SDT Q600 V20.9 Build 20 and heated from room temperature to 800 °C under air atmosphere at a rate of 10 °C min^{-1}.

A blue single crystal was carefully picked up from the mother liquor to collect data on a four-circle KUMA KM4 diffractometer which was equipped with a two-dimensional CCD area detector. The graphite-monochromatized MoKα radiation ($\lambda = 0.71073$ Å) and the ω-scan technique ($\Delta\omega = 1°$) were applied for data collection. Data was integrated using the CrysAlis software package [41]. To solve the structures, direct methods using SHELXS-97 were applied that determined the positions of almost all non-hydrogen atoms [42]. The other atoms were fixed with subsequent difference Fourier syntheses [43]. Using SHELXL-2014 with the anisotropic thermal displacement parameters, the materials were purified. The hydrogen atoms of the aromatic ring were refined with the riding model. The data was deposited in the Cambridge crystallographic data center with deposition number CCDC 1,911,460.

2.2. Synthesis single crystal of $[Cu_2(3,4\text{-pydc})_2(H_2O)_5]_n.2nH_2O$ (1)

Single crystals of 1 were grown by a three-layer diffusion method. A U-tube was third-filled with distilled water with a 2 ml methanolic solution of 0.1 mmol $Cu(OAc)_2.H_2O$ in the top of one arm and a 2 ml methanolic solution of 0.1 mmol 3,4-pyridinedicarboxylic acid and 0.2 mmol triethylamine in the other arm. The blue single crystals were formed after a week. They were filtered off, washed several times with water and dried under decreased pressure. Analytical calculations for $C_{14}H_{16}Cu_2N_2O_{13}.2H_2O$: H 3.43%, C 28.82%, N 4.80% and found: H 3.51%, C 28.69%, N 4.35%.

2.3. Sensitizing experiment

A suspension of compound 1 (1 *g*/L) was immersed in 1 mM aqueous solution of terbium nitrate and after soaking for a day, the precipitates were centrifuged and washed several times with water to eliminate adsorbed terbium(III) ions on the surface. Then, the solid-state fluorescence spectra of Tb^{3+}@1 ions were recorded at a 268 nm excitation wavelength of the organic ligand.

2.4. Sensing experiment

A suspension of compound 1 (2 g/L) was prepared by immersing 1 in deionized water under ultrasonic irradiation (1 h) to form a stable suspension afterward. The incorporated M^{n+}@1 were formed by mixing 1 ml of compound 1 suspension and 1 ml of the aqueous solution of diverse metal ions (1 mM) to investigate the fluorescence properties. Turn-on sensing of Tb^{3+}@1 as a function of Tb^{3+} ion concentration was assessed through the fluorescence measurements. Tb^{3+}@1 was obtained by mixing 1 ml of compound 1 suspension and 1 ml of Tb^{3+} aqueous solutions in different concentrations ranging from 20 μm to 1 mM. Time-dependent fluorescence turn-on of compound 1 in presence of the terbium ions was examined by adding compound 1 suspension (1 ml of 2 g/L) in 1 ml of Tb^{3+} aqueous solution (1 mM) and the fluorescence spectra of the mixture were recorded at different times (1, 2, 5, 10 and 15 min). To explore the interference effects of the other cations, 1 ml of compound 1 suspension was mixed in 1 ml aqueous solution containing Fe^{2+}, Cd^{2+}, Cr^{3+}, Mn^{2+}, Ca^{2+}, K^{+}, Ag^{+}, Na^{+}, Mg^{2+} and Al^{3+} cations (1 mM to each) and fluorescence of the mixture was measured.

2.5. Separation experiment

Separation experiments were carried out by adding 10 ml compound 1 suspension (2 *g*/L) to a 10 ml solution of terbium nitrate with concentrations varying from 200 to 600 μM. After a day, all of the precipitates were centrifuged, washed several times with water to remove excess Tb^{3+} ions and dried in the air to prepare samples for ICP-MS analyses.

2.6. Reusability test

Reusability test was accomplished *via* the following method. The precipitates of 1-Tb^{3+} were immersed in a water solution of copper nitrate (0.1 M) for one day, then the solid was separated from the solution, washed with water 5 times and the dried solid was used for reusability tests of terbium ions sensing.

3. Results and discussion

3.1. Crystal structure

Single crystals of $[Cu_2(3,4\text{-pydc})_2(H_2O)_5]_n.2nH_2O$ (1) were obtained by the layer diffusion crystal growth method from 3,4-pydc and $Cu(acetate)_2.H_2O$. The Crystal data analysis reveals that compound 1 is crystallized in the monoclinic space group $P2_1/c$ as a three-dimensional coordination polymer or metal-organic framework. Details of crystal data are presented in Table 1. The asymmetric unit includes three crystallographically independent copper ions (Fig. 1a). As shown in Fig. 1b each copper center experiences a different coordination environment. Cu1 is six-coordinated by three different 3,4-$pydc^{2-}$ anionic bridge ligands (three O atoms from two 3,4-$pydc^{2-}$ ligands and one N atom from the third 3,4-$pydc^{2-}$ ligand) and two coordinated water molecules, adopting disordered octahedral geometry. Cu2 is surrounded by four oxygen atoms from four coordinated water molecules and two oxygen atoms from two monodentate carboxylate groups of the two 3,4-$pydc^{2-}$ ligands. The octahedral environment of Cu3 is outlined by two nitrogens atoms of the two 3,4-$pydc^{2-}$ ligands in the axial position and four oxygen atoms in the equatorial positions are provided by the two monodentate carboxylate groups of the two 3,4-$pydc^{2-}$ ligands

Table 1
Crystal data and structure refinement details of compound 1.

Chemical formula	$C_{14}H_{16}Cu_2N_2O_{13}\cdot 2(H_2O)$
M_r	583.40
Crystal system, space group	Monoclinic, $P2_1/c$
Temperature (K)	100
a, b, c (Å)	7.0796 (7), 10.8188 (11), 24.8619 (19)
β (°)	90.734 (9)
V (Å^3)	1904.1 (3)
Z	4
Radiation type	Mo $K\alpha$
μ (mm^{-1})	2.32
Crystal size (mm)	0.22 × 0.07 × 0.06
Diffractometer	KUMA KM-4 with CCD detector
T_{min}, T_{max}	0.948, 1.000
No. of measured, independent and observed [$I > 2\sigma(I)$] reflections	25733, 6762, 3976
R_{int}	0.074
(sin θ/λ)$_{max}$ (Å^{-1})	0.773
$R[F^2 > 2\sigma(F^2)]$, $wR(F^2)$, S	0.057, 0.127, 1.00
No. of reflections	6762
No. of parameters	343
No. of restraints	21
H-atom treatment	H atoms treated by a mixture of independent and constrained refinement
Δ⟩$_{max}$, Δ⟩$_{min}$ (e Å^{-3})	1.05, -1.24

and two water molecules. The 3D structure of compound 1 has an interesting topology as exhibited in Fig. 2a and b, in which each Cu3 is connected to six Cu1 through four 3,4-pydc^{2-} ligands to generate a 3D porous network with two carboxylate functional groups directed towards inside the pores bonding in a monodentate fashion to the Cu2 atoms. This is shown in Fig. 2c where Cu2 atoms are bonded to the functional groups of linkers and cap the pores. The simplified structures are shown in Fig. 2 beneath their corresponding figures. The selected bonds and angles around copper centers are listed in Table 1S.

As presented in Table 2S, classical O-H…O hydrogen bonding between O6 and O7 of water guest molecules and three-dimensional metal-organic networks ranging from 2.688 to 3.207 Å and angles from 149 to 177° are responsible for host guest supramolecular architecture. Furthermore, there is a wide range of O-H…O classical hydrogen bonding between the coordinated water molecules and carboxylate groups and also C-H…O non-classical hydrogen bonding as intramolecular interactions in 1.

3.2. General characterization

PXRD of the synthesized compound 1 along with the simulated pattern from 1 single crystals' X-ray diffraction data, are presented in Fig. 3. The two patterns match well which confirms single phase purity of 1 (Fig. 3a and b). Furthermore, water stability of compound 1 was examined by treating this compound in boiling water for 4 h and as shown in Fig. 3c, the PXRD pattern of treated 1 proves its stability in water.

As presented in Fig. 4a, infrared spectrum of 1 shows a wide band in the 3000–3500 cm^{-1} region corresponding to the OHe stretching vibration mode of the water molecules in the 3D network. Appearing bands at 1623, 1571, 1419 and 1394 cm^{-1} confirm the coordination between carboxylate groups and copper ions which can be associated to asymmetric and symmetric stretching of coordinated carboxylate groups ν(COO-), respectively. The multiple IR absorption peaks of carboxylate group vibrations, confirm the different coordination modes of the carboxylate groups.

Thermal stability of 1 was inspected *via* thermal gravity analysis in the range of 50–800 °C. As shown in Fig. 5, TGA and DSC curves have three steps, the first step can be associated with the release of guest water molecules inside the pores. The result shows 1 is stable up to 250 and decomposition of the structure involves two exothermic steps. The decomposition takes place between 250 and 700 and the total weight loss is around 76% originating from the formation of CuO (calculated 73%).

3.3. Photoluminescence properties

Considering its special geometry, potential application as cationic exchange compound and the high chemical stability in water, compound 1 was studied for the detection of various cations based on fluorescent sensing in aqueous solutions. As shown in Fig. S1, both emission spectra of 3,4-H_2pydc and 1 exhibit a board band at 350 nm, upon excitation at 268 nm, which could be ascribed to the ligand-based π → π* transition. However, the fluorescence intensity of 1 is higher than that of the free ligand which could be attributed to the strong electronic communication of the coordinated ligands and Cu(II) ions (Fig. S1).

Solvent-dependent fluorescence property of 1 was investigated in diverse solvents to find the best solvent for the cation sensing system (Fig. 6). The suspension of compound 1 in water, Ethanol, Methanol, DMF, THF, DCM, and acetone shows solvent-dependent fluorescence emission intensity. The maximum fluorescence intensity was observed in water and ethanol and because of stability of 1 in the aqueous solution, water was chosen for all the sensing experiments.

The cation sensing measurements were carried out in a mixture

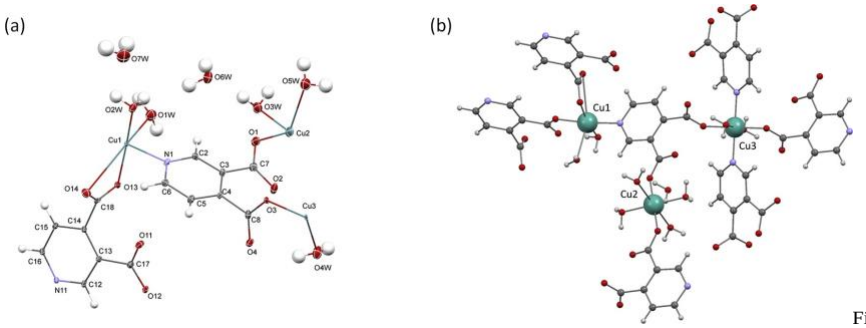

Fig. 1. (a) Asymmetric unit of 1 with the atom numbering scheme (b) The coordination environment of Cu(II) metal centers.

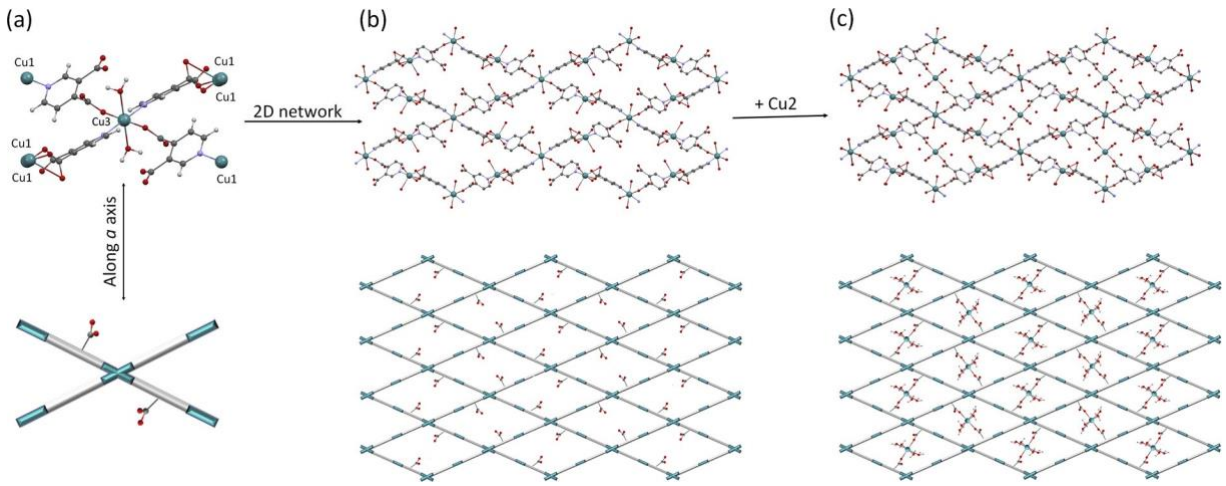

Fig. 2. (a) Coordination environment of Cu3 atoms, (b) 2D view of the 3D porous network of 1 along the *a* axis without and (c) with Cu2 atoms (simplified figures are shown beneath corresponding figures).

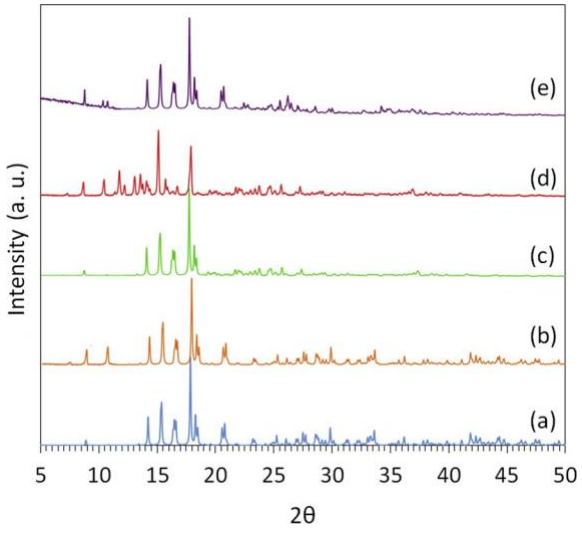

Fig. 3. (a) The simulated XRD pattern from compound 1 single crystals, (b) PXRD pattern of as synthesized bulk crystals of 1, (c) PXRD pattern of 1 after treating with boiling water, (d) PXRD pattern of Tb^{3+} @1 and (e) PXRD pattern of 1 after desorption.

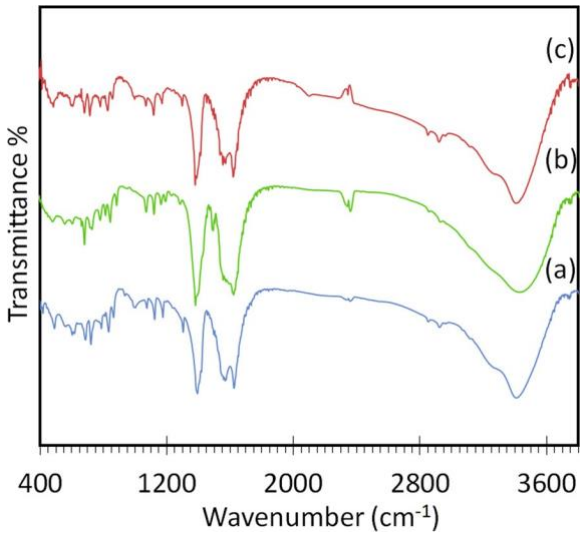

Fig. 4. IR spectra of 1: (a) bulk crystal as synthesized, (b) after Tb^{3+} ion adsorption, (c) the recovered 1.

the sensing and separation ability of compound 1 were examined through fluorescence studies and ICP-Mass spectroscopy for the different concentrations of Tb^{3+} ions in mixture with compound 1 suspensions.

3.4. Sensitizing and selective sensing of terbium ions

Sensitizing lanthanide ions incorporated into the metal-organic framework is of great interest due to their promising applications as optical materials. To explore sensitizing Tb^{3+} ions through the incorporation of Tb^{3+} ions into 1, a suspension of 1 was immersed in an aqueous solution of terbium nitrate and after soaking for a day, solid-state fluorescence spectra of Tb^{3+} @1 were recorded at a 268 nm excitation wavelength. As illustrated in Fig. S2, the emission spectrum shows characteristic emissions of Tb^{3+} ions and proves the antenna effect of the 3,4-$pydc^{2-}$ anionic ligand. PXRD of Tb^{3+}@1 confirms that the 3D network of 1 remains intact after inclusion of Tb^{3+} ions (Fig. 3d) and as shown in Fig. 3b, the FT-IR spectrum of Tb^{3+}@1 has a complicated pattern for carboxylate group vibrations in comparison with the spectrum for 1 which could be attributed to the coordination of carboxylate groups to Tb^{3+} ions.

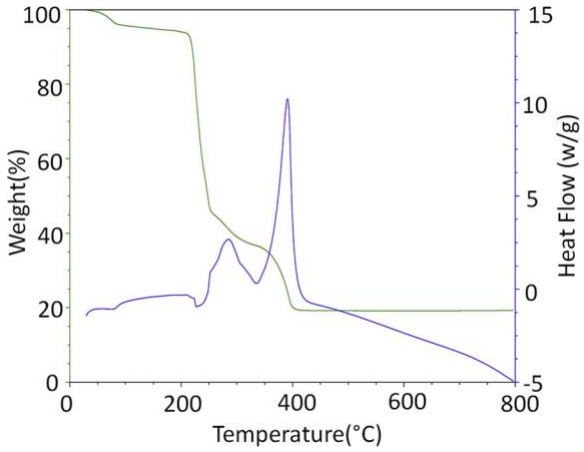

Fig. 5. TGA-DSC curve of 1.

To examine the ability of 1 for Tb^{3+} ions sensing, the fluorescence intensity of Tb^{3+}@1 in different concentrations of Tb^{3+} ions in the range of 20 μM-1 mM was recorded. As presented in Fig. 8, the

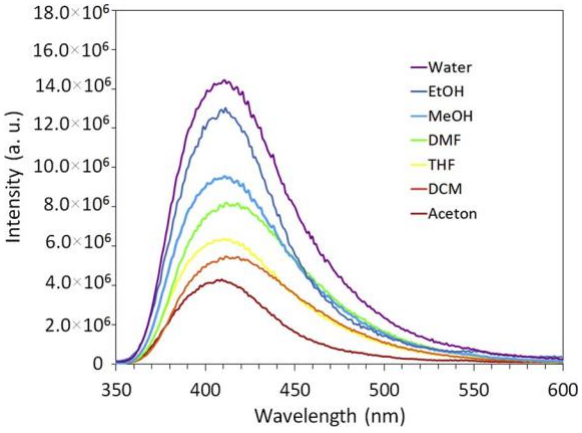

Fig. 6. Fluorescence spectra of 1 in different solvents upon excitation at 268 nm.

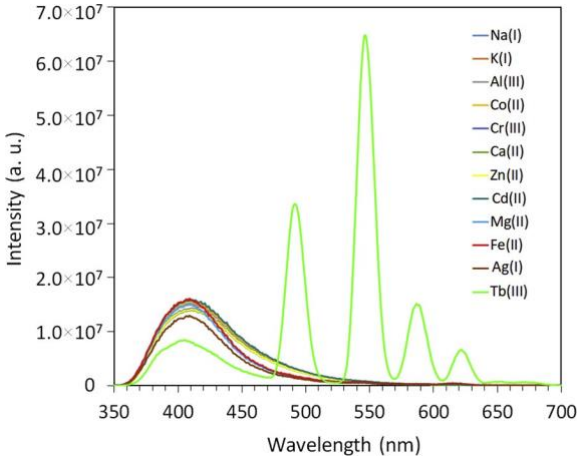

Fig. 7. Fluorescence spectra of 1 in the presence of diverse metal ions upon excitation at 268 nm.

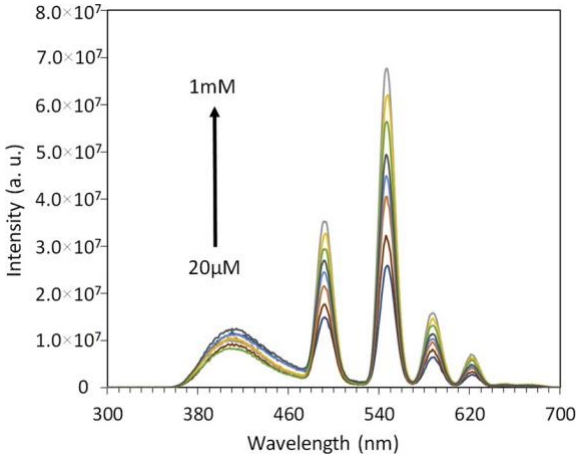

Fig. 8. Fluorescent spectra of Tb^{3+}@1 in water in the presence of different concentrations of Tb^{3+} ions upon excitation at 268.

fluorescent intensity of Tb^{3+} ions emissions are increased by increasing Tb^{3+} ions concentration, which confirms sensing ability of 1 towards Tb^{3+} ions. Time-dependency of fluorescence intensity of Tb^{3+}@1 is presented in Fig. 9. The results show that the intensity reaches its maximum value in 2 min and it confirms that the Tb^{3+} ions can diffuse to the network rapidly and interaction with linkers sensitizes their emission. In order to explore the detection selectivity of 1 towards Tb^{3+}

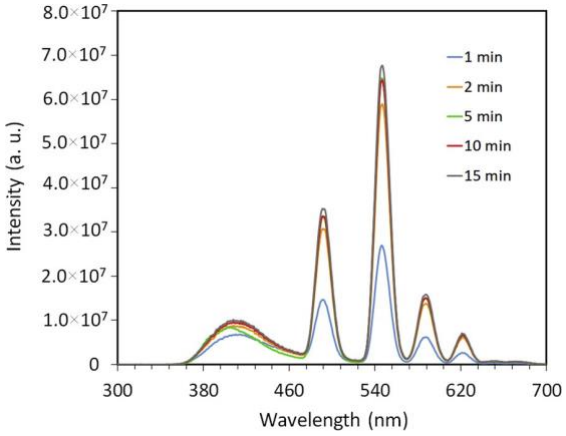

Fig. 9. Fluorescent spectra of Tb^{3+}@1 in water at different points of time upon excitation at 268 nm.

ions and examine the interference influence of other metal ions, the fluorescence spectra of a mixture of metal ions (1 mM for each ion) including 1 were recorded. As shown in Fig. S3, the fluorescence intensity of Tb^{3+}@1 in the mixture of metal ions is comparable with the emission of the Tb^{3+}@1 in the absence of other ions and the intensity is slightly decreased. Therefore, compound 1 demonstrated selective sensing for Tb^{3+} ions in the mixture of metal ions, which confirms it can be utilized as a sensor for luminescence sensing of Tb^{3+} ions.

3.5. *Separation of terbium*

To determine the chemical separation capability of 1 and the amount of Tb^{3+} ions that can be introduced into the copper framework, compound 1 was immersed in aqueous solutions of Tb^{3+} ions with different concentrations. As presented in the Table 3S, the ICP-MS results demonstrate that introducing the Tb^{3+} ions into the network resulted in reducing the copper content of the network. It can be concluded that the Tb^{3+} ions were inserted to the framework through a cationic exchange process and considering the topology of 1, the cation exchange took place with the copper ions residing inside the pores, which are weakly connected to the 3D porous network. Also, as mentioned before the PXRD pattern of 1 was relatively unchanged after adsorption and desorption of Tb^{3+} ions. Thus, the ICP-MS and PXRD results confirm the cationic exchange mechanism for the chemical adsorption and sensing of Tb^{3+} ions.

3.6. *Reusability*

Considering the cationic exchange mechanism for adsorption and sensing, Tb^{3+}@1 was immersed into a concentrated copper(II) aqueous solution to examine cation exchange based on Le Chatlier's principle. The ICP-MS results of the recovered 1 confirm that the elimination of Tb^{3+} ion was taken place and Tb^{3+} ion adsorption is reversible in the presence of the concentrated copper(II) aqueous solution. Furthermore, the PXRD pattern of recovered 1 is almost identical to that of the original 1 pattern (Fig. 3e). The recovered 1 was utilized for sensing of Tb^{3+} ions and this cycle was repeated for five times. The results revealed that the emission intensity of Tb^{3+} ions remains constant during cycles and it confirms that 1 can be utilized as a long-term sensor and adsorbent for Tb^{3+} ions.

4. Conclusion

In summary, we have reported a novel 3D porous network of copper with a special topology, with Cu2 ions inside the pores enabling its potential application as a cationic exchange compound. Our research is

pivoted around applications of 1 in sensitizing, sensing and chemical separation of Tb^{3+}ions, which collectively have the potential to address the environmental issues associated with these ions. Compound 1 exhibited efficient sensitizing and sensing ability for Tb^{3+} ions and can also selectively absorb Tb^{3+} ions from the mixture of cations. The efficient sensitizing, sensing, selective adsorption and reusability demonstrate that 1 can be utilized as a long-term sensor and adsorbent for Tb^{3+} ions.

Declaration of Competing Interest

The authors declare no conflict of interest.

Acknowledgement

The authors thank the University of Tehran for the supports.

Appendix A. Supplementary data

Supplementary material related to this article can be found, in the online version, at doi:https://doi.org/10.1016/j.materresbull.2019.110683.

References

[1] X. Zhao, M. Wong, C. Mao, T.X. Trieu, J. Zhang, P. Feng, X. Bu, J. Am. Chem. Soc. 136 (2014) 12572–12575.
[2] S. Iftekhar, D.L. Ramasamy, V. Srivastava, M.B. Asif, M. Sillanpää, Chemosphere 204 (2018) 413–430.
[3] W. Hua, T. Zhang, M. Wang, Y. Zhu, X. Wang, Chem. Eng. J. 370 (2019) 729–741.
[4] X. Huang, J. Dong, L. Wang, Z. Feng, Q. Xue, X. Meng, Green Chem. 19 (2017) 1345–1352.
[5] Ó. Barros, L. Costa, F. Costa, A. Lago, V. Rocha, Z. Vipotnik, B. Silva, T. Tavares, Molecules 24 (2019) 1005.
[6] J.E. Quinn, K.H. Soldenhoff, G.W. Stevens, Hydrometallurgy 169 (2017) 621–628.
[7] E. Kashi, R. Habibpour, H. Gorzin, A. Maleki, J. Rare Earths 36 (2018) 317–323.
[8] X. Xu, X.-Y. Jiang, F.-P. Jiao, X.-Q. Chen, J.-G. Yu, J. Taiwan Inst. Chem. Eng. 85 (2018) 106–114.
[9] E. Liu, X. Zheng, X. Xu, F. Zhang, E. Liu, Y. Wang, C. Li, Y. Yan, New J. Chem. 41 (2017) 7739–7750.
[10] W. Zhang, R.Q. Honaker, Int. J. Coal Geol. 195 (2018) 189–199.
[11] T. Suzuki, M. Tanaka, Y. Ikeda, S.I. Koyama, J. Radioanal. Nucl. Chem. 296 (2013) 289–292.
[12] S. Harika, P. Niharika, N. Srinath, K. Vijay, Int. J. Pharm. Technol. 3 (2011) 1696–1708.
[13] C.M. Babu, K. Binnemans, J. Roosen, Ind. Eng. Chem. Res. 57 (2018) 1487–1497.
[14] J. Florek, F. Chalifour, F. Bilodeau, D. Larivière, F. Kleitz, Adv. Funct. Mater. 24 (2014) 2668–2676.
[15] J. Florek, D. Larivière, F. Kleitz, ACS Symposium Series (2016) 107–117.
[16] S. Yuan, L. Feng, K. Wang, J. Pang, M. Bosch, C. Lollar, Y. Sun, J. Qin, X. Yang, P. Zhang, Q. Wang, L. Zou, Y. Zhang, L. Zhang, Y. Fang, J. Li, H.-C. Zhou, Adv. Mater. 30 (2018) 1704303.
[17] H. Furukawa, K.E. Cordova, M. O'Keeffe, O.M. Yaghi, Science 341 (2013) 1230444.
[18] V.R. Remya, M. Kurian, Int. Nano Lett. 9 (2019) 17–29.
[19] V.F. Cheong, P.Y. Moh, Mater. Sci. Technol. 34 (2018) 1025–1045.
[20] Q. Qiu, H. Chen, Y. Wang, Y. Ying, Coord. Chem. Rev. 387 (2019) 60–78.
[21] X. Zhang, G. Li, D. Wu, X. Li, N. Hu, J. Chen, G. Chen, Y. Wu, Biosens. Bioelectron. 137 (2019) 178–198.
[22] L. Joseph, B.M. Jun, M. Jang, C.M. Park, J.C. Muñoz-Senmache, A.J. Hernández-Maldonado, A. Heyden, M. Yu, Y. Yoon, Chem. Eng. J. (2019) 928–946.
[23] A. Karmakar, P. Samanta, A.V. Desai, S.K. Ghosh, Acc. Chem. Res. 50 (2017) 2457–2469.
[24] L. Li, S. Shen, W. Ai, S. Song, Y. Bai, H. Liu, Sens. Actuators B Chem. 267 (2018) 542–548.
[25] D. Kukkar, K. Vellingiri, K.-H. Kim, A. Deep, Sens. Actuators B Chem. 273 (2018) 1346–1370.
[26] L.E. Kreno, K. Leong, O.K. Farha, M. Allendorf, R.P. Van Duyne, J.T. Hupp, Chem. Rev. 112 (2012) 1105–1125.
[27] P. Kumar, A. Deep, K.-H. Kim, TrAC Trends Anal. Chem. 73 (2015) 39–53.
[28] X. Fang, B. Zong, S. Mao, Nano-Micro Lett. 10 (2018) 64.
[29] Y. Cui, Y. Yue, G. Qian, B. Chen, Chem. Rev. 112 (2012) 1126–1162.
[30] B. Chen, S. Xiang, G. Qian, Acc. Chem. Res. 43 (2010) 1115–1124.
[31] M.D. Allendorf, C.A. Bauer, R.K. Bhakta, R.J.T. Houk, Chem. Soc. Rev. 38 (2009) 1330–1352.
[32] Y.D. Farahani, V. Safarifard, J. Solid State Chem. 275 (2019) 131–140.
[33] Y. Zhang, B. Yan, Talanta 197 (2019) 291–298.
[34] S. Senthilkumar, R. Goswami, V.J. Smith, H.C. Bajaj, S. Neogi, ACS Sustain. Chem. Eng. 6 (2018) 10295–10306.
[35] Y. Su, J. Yu, Y. Li, S.F.Z. Phua, G. Liu, W.Q. Lim, X. Yang, R. Ganguly, C. Dang, C. Yang, Y. Zhao, Commun. Chem. 1 (2018) 12.
[36] S. Chen, F. Feng, S. Li, X.-X. Li, L. Shu, Chem. Speciat. Bioavailab. 30 (2018) 99–106.
[37] J. Hu, K. Wu, S. Dong, M. Zheng, Polyhedron 153 (2018) 261–267.
[38] J.J. Liu, L.M. Yu, F.X. Han, F.Y. Chen, F.X. Cheng, J. Solid State Chem. 270 (2019) 45–50.
[39] Q. Zhang, J. Wang, A.M. Kirillov, W. Dou, C. Xu, C. Xu, L. Yang, R. Fang, W. Liu, ACS Appl. Mater. Interfaces 10 (2018) 23976–23986.
[40] E.-L. Zhou, C. Qin, D. Tian, X.-L. Wang, B.-X. Yang, L. Huang, K.-Z. Shao, Z.-M. Su, J. Mater. Chem. C 6 (2018) 7874–7879.
[41] Oxford Diffraction Poland, CrysAlis CCD and CrysAlis Red, Version 1.171.33.42, Wrocław, Poland (2009).
[42] George Michael Sheldrick, SHELXS97, Programs for Crystal Structures Solution and Refinement, University of Göttingen, Göttingen, Germany, 1997.
[43] G.M. Sheldrick, Acta Crystallogr. C71 (2015) 3–8.